Effects of Zirconia Shot Peening on High Cycle Fatigue Properties of Ti-6Al-4V Alloy

K. Masaki[1], N. Hisamori[2], Y. Kobayashi[3] and D. Gowa[3]

1 Okinawa National College of Technology, Nago, Okinawa, JAPAN
2 Sophia University, Chiyoda, Tokyo, JAPAN
3 SINTOKOGIO LTD, Nagoya, Aichi, JAPAN

Abstract
Cantilever type rotating bending fatigue tests were conducted in order to investigate the effects of shot peening treatment on the fatigue properties of a Ti-6Al-4V titanium alloy. Shot peening was performed with three types of fine zirconia shot grids with different diameters and material grades. The fatigue lives of shot peened specimens fractured from the inside with a fish eye on the fracture surface were longer than those of non-peened specimens fractured from the surface. To discuss the fatigue properties, the fracture surfaces were observed and the peening effects such as surface roughness, hardness and residual stress were examined. From the observation of fish eye patterns on the fracture surfaces, it was clear that the residual stress influenced the fatigue properties of Ti-6Al-4V greatly.

Keywords: Fatigue property, Ti-6Al-4V alloy, Shot peening, High cycle fatigue, Fish-eye.

Introduction
Ti-6Al-4V is the most popular titanium alloy used for aerospace industrial components [1, 2] and for biomedical materials [3-5] because it has superior corrosion property and high tensile strength at high temperature. In many cases, cyclic load acts the components while they are used, so the improvement of the high cycle fatigue property is necessary to enhance the reliability of components. Though improving the yield strength of material is effective to increase the fatigue limit, the fatigue life is not necessarily always extended because the toughness of the material falls down. In this report, shot peening treatment with fine zirconia shot grids was applied in order to improve the fatigue lives of Ti-6Al-4V in which three types of fine zirconia shot grids with different diameters and material grades. Cantilever type rotating bending fatigue tests were conducted in order to investigate the effects of the shot peening treatment on the fatigue property in the work-hardened Ti-6Al-4V titanium alloy which had higher tensile strength and fatigue limit than those of usual Ti-6Al-4V material.

Experimental Procedure
Material and Fatigue Specimens: Material used in this study is Ti-6Al-4V titanium alloy prepared through hot working. Before machining, solution heat treatment, water cooling after holding 60 min. at 960 ℃ and air cooling after holding 360 min. at 550 ℃, were applied. Table 1 shows chemical compositions and Table 2 shows mechanical properties of the material. One of characteristics of this material is that the yield stress is comparably high, i.e., about 94% of the Tensile strength. Figure 1 exhibits the microstructure on the cross and longitudinal sections of the material, showing a bimodal structure of α-Ti and α+β-Ti without any anisotropy. Figure 2 shows the shape of fatigue test specimens, which is a simple hour

Table 1 Chemical composition [wt%]

Ti	Al	V	O	Fe	C	N	H
Bal	6.14	4.06	0.17	0.15	0.01	<0.01	0.01

Table 2 Mechanical properties

Tensile strength [MPa]	Yield stress [MPa]	Elongation [%]
1178	1107	8.4

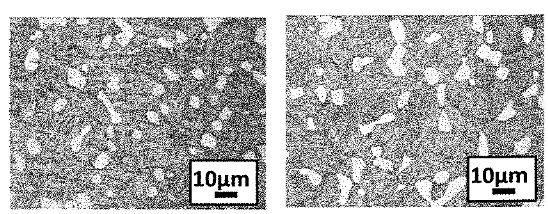

(a) Cross section (b)Longitudinal section

Fig.1 Microstructure of material.

glass type with a shallow notch of 4 mm minimum diameter on a rod of 12 mm diameter. The stress concentration factor is 1.07 [6]. After machining, the surface of the shallow notch was mirror finished by emery paper and buff cloth with alumina liquid of 1μm and 0.1μm diameter.

Shot Peening Conditions:
Shot peening was conducted with three types of fine zirconia shot grids. Figure 3 shows macro photograph of shot grids. The average diameter of B120 grids is about 0.12mm and those of Z300 and Y300 grids are 0.3 mm. Difference between Z300 and Y300 is material grades. The grade of Y300 is higher than Z300. Table 3 shows shot peening conditions. All shot peening treatments were conducted under mild conditions by an air type shot peening machine. The air pressure of all treatments is 0.5 MPa. The Almen intensities of the treatments were between 0.2 and 0.35 mmN.

Fatigue Tests and Fracture Surface Observation:
High cycle fatigue tests were conducted with a cantilever type rotating bending fatigue testing machine in air at room temperature. The stress ratio is R= -1 and the rotation speed of the spindle is 3600 rpm. After the fatigue fracture of specimens, all fracture surfaces were observed by a stereoscopic microscope and a scanning electron microscope, SEM, in order to investigate the fatigue crack initiation site.

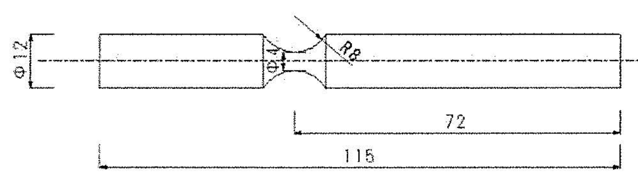

Fig.2 Configuration of fatigue specimens, mm.

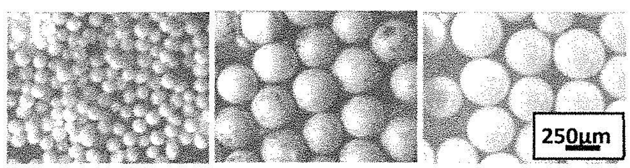

(a) B120 **(b) Z300** **(c) Y300**
Fig.3 Shot grids.

Table 3 Conditions of shot peening.

Shot material	B120	Z300	Y300
Shot diameter [mm]	0.12	0.3	0.3
Peening time [s]	24	24	32
Arc Height [mmN]	0.205	0.310	0.352
Air Pressure [MPa]		0.5	

Results and Discussion

Fatigue Results:
Figure 4 shows the S-N diagram of fatigue testing results of all materials. Examples of the fracture surfaces observed by SEM are shown in Figs. 5 and 6. The open symbols in Fig. 4 represent the fatigue cracks initiated from the surface of the specimens as shown in Fig.5. On the other hand, solid symbols stand for cracks initiated from inside the specimen. Fish eye patterns were evidently observed on the fracture surfaces of almost all internally-fractured specimens as shown in Fig. 6, however there are no clear patterns on the two specimens marked with '☆' in Fig. 4. All specimens of the non-peened material fractured from the surfaces and the fatigue limit was about 700MPa. On the other hands, the fracture type of shot peened specimens depends on the shot peening conditions: The specimens fractured from the surfaces when stress amplitude was high whereas they fractured from the inside when stress amplitude is low. The fracture type changes at a stress amplitude of about 850MPa in Z300 and Y300, and about 950MPa in B120. The fatigue lives of shot peened specimen fractured from the surfaces are the same level as those of non-peened specimens. On the other hand, fatigue lives of shot peened specimens with internal fracture are longer than those with surface fracture. The fatigue life of B120 is the longest and it is about hundred times longer compared to that of non-peened specimens. And then, the fatigue lives of Z300 and Y300 are in the same level and they are about ten times longer than those of specimens with surface fracture.

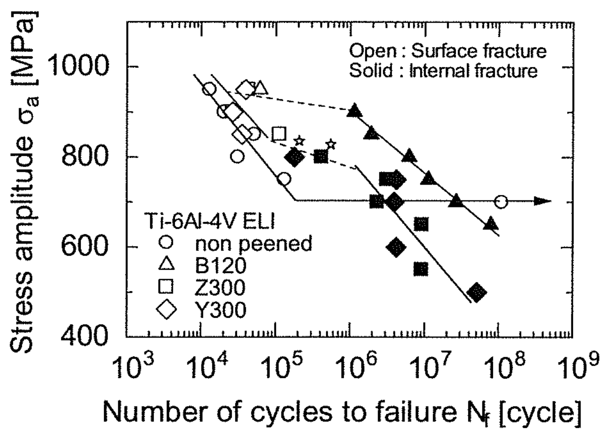

Fig.4 S-N diagram of fatigue results.

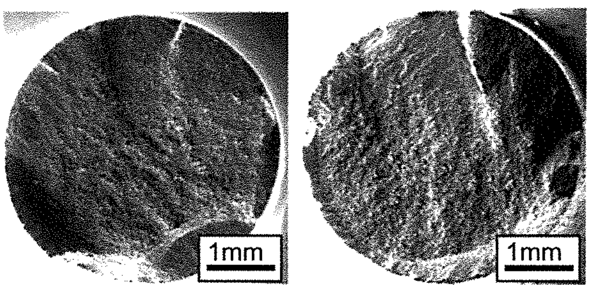

(a) n.p. 900MPa (2.04×10^4cycle) (b) Z300 900MPa (2.63×10^4cycle)

Fig.5 Fracture surface (surface origin type).

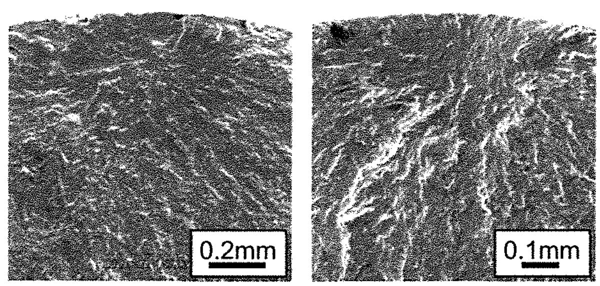

(a) Y300 750MPa (4.17×10^6cycle) (b) B120 650MPa (7.87×10^7cycle)

Fig.6 Fracture surface (Internal origin type).

Peening effects: Increase in surface roughness is one of the negative effects accompanied by shot peening for improving fatigue properties. Especially, since Titanium alloy is a high notch-sensitive material, the negative effect due to the increase in surface roughness would be prominent. At first, the change of surface roughness profile by shot peening was investigated. Table 4 shows the surface roughness of all specimens, showing increases by shot peening. Here, 'Ra' is 'Average roughness', 'Ry' is 'Maximum height' and 'Rz' is '10-point average roughness' over the length of 4 mm. Rz of B120, Z300 and Y300 after shot peening are about 7.6, 7.4 and 10.8 times greater compared with non-peened materials. Although surface roughnesses are the same level between B120 and Z300, there is a great difference in fatigue property as shown in Fig.4.

Next, hardness increase which is one of the major peening effects was investigated using a Vickers hardness tester. Figure 7 shows hardness distribution in every 0.02mm of all specimens from the surface to a depth of 1mm. Here, hardness measuring conditions were 0.98N and 15sec. The hardness of Ti-6Al-4V matrix is about 370HV. The hardness of the specimen surface depends on the specimens. Surface hardening of the non-peened specimen was about 450HV. There may be an effect by machine processing when making specimens. The surface hardnesses of Z300, Y300 and B120 were 495Hv, 510Hv and 460Hv, respectively. Although the surface hardnesses are in the same level between non-peened specimen and B120, there is a great difference in the fatigue property as shown in Fig.4. In addition, although the surface hardnesses of Y300 and Z300 are higher than that of B120, fatigue lives of Z300 and Y300 are shorter than that of B120. As a result, it would be considered that the effect of the hardness increase by peening on the fatigue property was small in Ti-6Al-4V material used in this study.

Finally, residual stress distributions near the surface of all types of specimens were investigated. Residual stress was measured by X-ray diffraction (XRD) with Cu-Kα radiation (50kV, 30mA) applying the $\sin^2\psi$-method on the {213}-plane of the hexagonal α-phase Ti and K= -217 MPa/deg as a stress constant [7]. Figure 8 shows residual stress distributions obtained by repeating the XRD measurement and electrolytic polishing, alternately. In all types of specimens, compressive residual stress exists on the surface. The largest compressive residual stress was about 1150 MPa on B120. The profiles of residual stress distribution are similar between the Z300 and the Y300, and the compressive residual stresses on the surface are about 750MPa. For all peened specimens, high compressive residual stresses over 400MPa exist inside the specimens deeper than 15μm. On the other hand, the compressive residual stress on the surface of non-peened specimens is about 500MPa, but it exists only within a thin surface layer.

Table 4 Surface roughness values

	Ti-6Al-4V	Shot processed		
	Mirror finish	B120	Z300	Y300
Ra[μm]	0.15	0.72	0.88	1.43
Ry[μm]	0.8	5.2	6.1	7.7
Rz[μm]	0.5	3.8	3.7	5.4

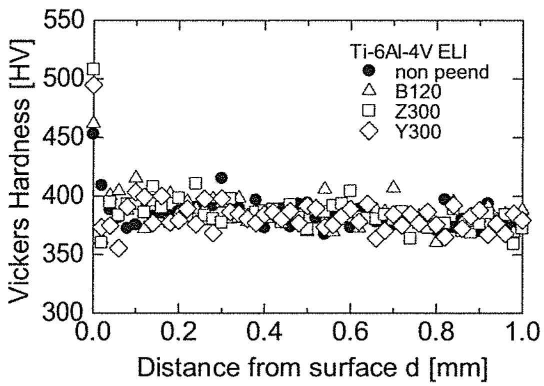

Fig.7 Vickers hardness distributions.

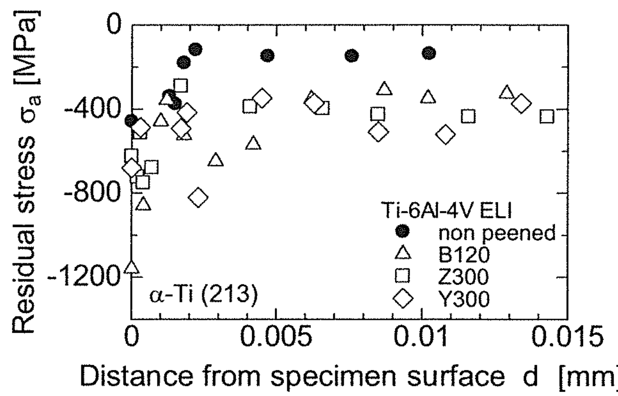

Fig.8 Residual stress distributions.

Peening conditions and fish eye:

Since fish eye formation is actively involved with fatigue loading cycles, the characteristics of fish eye shape are investigated. Figure 9 shows the relationships between the stress amplitude of the fatigue test and the area of the fish eye. The area becomes larger as the stress amplitude becomes lower. Only B120 has different propensity to Z300 and Y300. The area of the fish eye of B120 is dominantly smaller than those of Y300 and Z300 at the same stress level. And generally, the area becomes larger as the fatigue life becomes longer, but the area of B120 is clearly smaller than those of Y300 and Z300.

Next, in order to investigate the fatigue crack propagation behavior, the relationship between the shape of the fish eye and the depth of crack initiation site is focused. Figure 10 shows the relationships between the depth of crack initiation site “d” and the radius ration “rs/rc”. The fatigue crack initiation site of B120 was located in a shallower position compared with Z300 and Y300. The depth of B120 crack initiation site is about 70μm and those of Z300 and Y300 are about 150μm. And then, there is a large difference in rs/rc of B120 and Z300 or Y300. The rs/rc values of B120 are distributed between 0.5 and 0.8. It means that fatigue crack propagates toward the surface preferentially than the center. On the other hand, the values of rs/rc are distributed between 0.25 and 0.55 in Z300 and Y300. In fact, in Z300 and Y300, the fatigue crack propagates toward the center preferentially than the surface. From this result, it is clearly that the fatigue fracture mechanisms are different between B120 and Z300 or Y300. In order to investigate this reason, the crack initiation site of the fish eye was observed with SEM in detail. Observation results are shown in Fig.11. Both crack initiation sites of Z300 and Y300 are similar in appearance each other and there is a trans-granular cracking on center part of the fish eye, called a "facet". Many papers on high cycle fatigue property of Ti-6Al-4V have also described the relation between the facet and crack generation [8-10].The facet size is about 10 to 20μm and is almost same as the size of α-Ti grains in matrix. On the other hand, there is no facet on the center part of the fish eye in B120. Instead, there is a fine granular area at the center part of the fish eye. For these reasons, it is considered that there is a difference in fatigue crack initiation mechanism between B120 and Z300 or Y300.

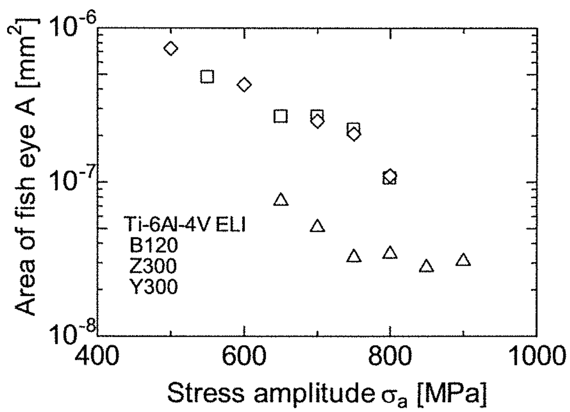

Fig.9 Relationship between σ_a and area of fish-eye.

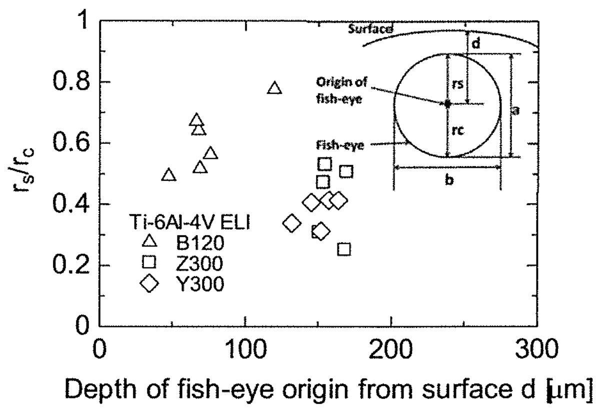

Fig.10 Relationship between d and rs / rc.

Fracture Mechanism of SP specimens:

Because the facet was generated at crack initiation site and the fatigue crack propagated toward the center preferentially, it would be considered that the area located at about 150μm depth from the surface had been subjected to a high level tensile stress in Z300 and Y300. When the fatigue crack tip of the fish eye reached to the specimen surface, the fish eye has enough grown inside the specimen. Accordingly, the specimen will fatigue fracture soon.

However, in B120, high level tensile stress required for facet formation does not act inside specimen. In B120, not a facet but a fine granular area was observed at the center part of the fish eye. Nakamura et al. have indicated that this fine granular area is formed by the repetition of high compressive stresses over a long period [11-12]. After the fine granular area formation, the fatigue crack propagated toward surface direction preferentially and the crack tip reached the specimen surface soon. Although the crack tip has reached to the surface, the surface fatigue crack propagates slowly because the stress intensity factor of the small fish eye is low. And the fatigue crack would be prevented by a high level compressive residual stress. It is considered that the cause of the long life of B120 is an extension of crack initiation cycles and a deceleration of the surface crack propagation rate.

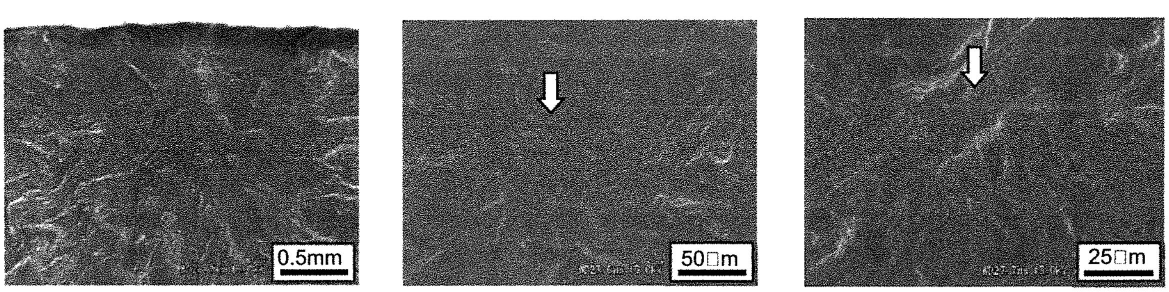

(a) B120 750MPa 1.12×10⁷ cycle (b) Z300 650MPa 9.26×10⁶ cycle (c) Y300 700MPa 3.92×10⁶ cycle

Fig.11 Magnification image of center part of fish eye.

It's considered that the cause of the difference in the fish eye formation mechanism between B120 and Z300 or Y300 is the difference in residual stress distributions introduced by the shot peening treatment. It is necessary to investigate the compressive residual stress distributions for all SP conditions more in detail.

Conclusions

Rotating bending fatigue testing of Ti-6Al-4V material was performed to investigate the effects of shot peening with three types of fine zirconia shot, B120, Z300 and Y300. The results are summarized as follows:

(1) The fatigue life of Ti-6Al-4V material can be extended by fine zirconia shot peening. But fatigue limit falls by shot peening.

(2) The extension of fatigue lives is most predominant through shot peening of zirconia shot grid B120, the smallest shots of about 0.12 mm diameter.

(3) The internal fracture with a fish eye occurred in all of the shot peened material under any conditions. There is a difference in fish eye formation mechanism between B120 and Z300 or Y300.

(4) Residual stress introduced by peening has largest effect on fatigue properties. The influence of hardness increase and surface roughness is relatively small.

References

[1] R.R. Boyer, *An overview on the use of titanium in the aerospace industry*, Materials Science and Engineering Vol.A213 (1996) pp.103-114.

[2] R.O. Ritchie, B.L. Boyce, J.P. Campbell, O. Roder, A.W. Thompson and W.W. Milligan, *Thresholds for high-cycle fatigue in a turbine engine Ti–6Al–4V alloy*, International Journal of Fatigue Vol.21 (1999) pp.653–662.

[3] L.R. Saitova, H.W. Höppel, M. Göken, I.P. Semenova and R.Z. Valiev, *Cyclic deformation behavior and fatigue lives of ultrafine-grained Ti-6AL-4V ELI alloy for medical use*, International Journal of Fatigue Vol.31 (2009) pp.322–331.

[4] B. Hamilton, S. Oppenheimer, D. C. Dunand and D. Lewis, *Diffusion Bonding of Ti-6Al-4V Sheet with Ti-6Al-4V Foam for Biomedical Implant Applications*, Metallurgical and Materials Transactions B, Vol.44 (2013) pp.1554–1559.

[5] T. Hanaka, *Biocompatibility of titanium - favorable properties*, Journal of The Japan Institute of Light Metals, Vol.62 (2012) pp.285–290.

[6] W. D. Pilkey, D. F. Pilkey, Peterson's Stress Concentration Factors, John Wiley & Sons, inc. (2007)

[7] N. Tsuji, S. Tanaka and T. Takasugi, *Effects of combined plasma-carburizing and shot-peening on fatigue and wear properties of Ti–6Al–4V alloy*, Surface & Coatings Technology Vol.203 (2009) pp.1400–1405.

[8] S. K. Jha, C. J. Szczepanski, P. J. Golden, W. J. Porter III and R. John, *Characterization of fatigue crack-initiation facets in relation to lifetime variability in Ti–6Al–4V*, International Journal of Fatigue, Vol.42 (2012) pp.248–257.

[9] J.H. Zuo, Z.G. Wang and E.H. Han, *Effect of microstructure on ultra-high cycle fatigue behavior of Ti–6Al–4V*, Materials Science and Engineering, Vol. A473 (2008) pp.147–152.

[10] I. Bantounas, D. Dye and T. C. Lindley, *The effect of grain orientation on fracture morphology during high-cycle fatigue of Ti–6Al–4V*, Acta Materialia, Vol.57 (2009) pp.3584–3595.

[11] H. Oguma, T. Nakamura, S. Yokoyama and T. Noguchi, *Very high cycle fatigue properties and fracture types of Ti-6A1-4V alloy*, Journal Society Material Science, Japan, Vol.52,(2003), pp.1298-1304.

[12] H. Oguma and T. Nakamura, *Fatigue crack propagation properties of Ti–6Al–4V in vacuum environments*, International Journal of Fatigue, Vol.50,(2013) pp.89–93.